Rapid synthetic routes to prepare $LiNi_{1/3}Mn_{1/3}Co_{1/3}O_2$ as a high voltage, high-capacity Li-ion battery cathode material

M. Sathiya [a], A.S. Prakash [a], K. Ramesha [a], A.K. Shukla [b,*]

[a] Central Electrochemical Research Institute, Karaikudi-630 006, Tamil Nadu, India
[b] Solid State and Structural Chemistry Unit, Indian Institute of Science, Bangalore-560 012, India

ARTICLE INFO

ABSTRACT

$LiNi_{1/3}Mn_{1/3}Co_{1/3}O_2$, a high voltage and high-capacity cathode material for Li-ion batteries, has been synthesized by three different rapid synthetic methods, viz. nitrate-melt decomposition, combustion and sol–gel methods. The first two methods are ultra rapid and a time period as small as 15 min is sufficient to prepare nano-crystalline $LiNi_{1/3}Mn_{1/3}Co_{1/3}O_2$. The processing parameters in obtaining the best performing materials are optimized for each process and their electrochemical performance is evaluated in Li-ion cells. The combustion-derived $LiNi_{1/3}Mn_{1/3}Co_{1/3}O_2$ sample exhibits large extent of cation mixing (10%) while the other two methods yield $LiNi_{1/3}Mn_{1/3}Co_{1/3}O_2$ with cation mixing <5%. $LiNi_{1/3}Mn_{1/3}Co_{1/3}O_2$ prepared by nitrate-melt decomposition method exhibits superior performance as Li-ion battery cathode material.

1. Introduction

Layered $LiCoO_2$ is widely used in commercial Li-ion batteries due to its high stability during electrochemical cycling, superior capacity and ease of preparation in bulk quantities [1–3]. However, high cost and toxicity of cobalt have pushed extensive research on nickel- and manganese-based lithium oxides as alternative cathodes. In this context, $LiNiO_2$ and $LiMn_2O_4$ have gained great interest and are being extensively studied as possible alternatives [4–6]. Further layered $LiMnO_2$ which has been synthesized via ion exchange from $NaMnO_2$ is also been studied as an alternate cathode material, however, it transforms to $LiMn_2O_4$ on cycling [7,8]. $LiNiO_2$ has a layered structure similar to $LiCoO_2$ with some amount of Ni present in 2+ oxidation state [4,5]. The nearly similar ionic radii for Ni^{2+}(0.69 Å) and Li^+(0.76 Å) make $LiNiO_2$ amenable to inter-layer cation-exchange [4,5]. This causes difficulty in its synthesis and also induces instability during cycling. Layered $LiMnO_2$ is thermodynamically less stable while spinel $LiMn_2O_4$ has the disadvantage of poor theoretical capacity with capacity fading during cycling [9]. Thus nickel and manganese-based compounds possessing $LiCoO_2$-type layered structure have inherent advantages, and are being considered as promising alternative to $LiCoO_2$ for large-scale applications.

The solid solution of $LiNiO_2$, $LiMnO_2$ and $LiCoO_2$ having composition $Li[Co_{1/3}Mn_{1/3}Ni_{1/3}]O_2$ has structure akin to α-$NaFeO_2$ [10]. It has a layered structure (space group: $R\bar{3}m$) with Li-ions located in-between the alternate layers of edge-shared MO_6 octahedra [11,12]. Ni^{2+} and Co^{3+} involve in the electrochemical process while Mn^{4+} with very high activation barrier for cation movement through tetrahedral site acts like a pillar to stabilize the structure during cycling [13]. Accordingly, $LiNi_{1/3}Mn_{1/3}Co_{1/3}O_2$ can be safely used in the voltage range between 2.3 and 4.5 V and even at higher voltages by combining with a suitable electrolyte. However, synthetic conditions do have strong influence on the electrochemical performance of $LiNi_{1/3}Mn_{1/3}Co_{1/3}O_2$ [14–16]. Low-temperature synthesis result in electrochemically less active spinel-like phase [17] while high-temperature syntheses lead to excess lithium loss and cation mixing [18]. Accordingly, it is always desirable to find optimum temperature and time duration for the synthesis of $LiNi_{1/3}Mn_{1/3}Co_{1/3}O_2$.

Various synthetic methods have been reported for the synthesis of $LiNi_{1/3}Mn_{1/3}Co_{1/3}O_2$, such as ceramic methods [19], acetate decomposition method [20], hydroxide precipitation method [21], carbonate co-precipitation method [22], etc. These methods have led to electrochemically active $LiNi_{1/3}Mn_{1/3}Co_{1/3}O_2$ phase but it becomes mandatory to heat the samples at 700–1000 °C for long durations to obtain good electrochemical performance.

In this paper, we report the synthesis of $LiNi_{1/3}Mn_{1/3}Co_{1/3}O_2$ using three different rapid synthetic methods, namely nitrate-melt decomposition, combustion and sol–gel method. Structural, morphological and electrochemical properties of the samples

* Corresponding author. Tel.: +91 80 22932795; fax: +91 80 23601310.
E-mail address: akshukla2006@gmail.com (A.K. Shukla).

have been studied and the synthetic conditions for each process are optimized to obtain the desired results. The nitrate-melt decomposition route [23] used here is novel and different from typical nitrate solution synthesis reported in the literature [24]. The method is simple and hence cost effective for synthesizing $LiNi_{1/3}Mn_{1/3}Co_{1/3}O_2$ in bulk.

2. Experimental

2.1. Synthesis of $LiNi_{1/3}Mn_{1/3}Co_{1/3}O_2$ by nitrate-melts decomposition

Powder samples of $LiNi_{1/3}Mn_{1/3}Co_{1/3}O_2$ were prepared by rapidly heating the mixture of $LiNO_3$, $Co(NO_3)_2·6H_2O$, $Ni(NO_3)_2·6H_2O$ and $Mn(NO_3)_2·4H_2O$ in the molar ratio of 1.05:0.33:0.33:0.33. The final lithium to transition-metal ratio was 1:1. In a typical preparation stoichiometric amounts of metal nitrates, viz. 7.2398 g of $LiNO_3·H_2O$, 9.6937 g of $Ni(NO_3)_2·6H_2O$, 8.367 g of $Mn(NO_3)_2·4H_2O$, 9.7013 g of $Co(NO_3)_2·6H_2O$, were taken in a sintered alumina crucible and introduced to a preheated furnace at 500 °C. The furnace was rapidly heated to 800 °C with a heating rate of 50 °C/min and allowed to stay for 15 min. Subsequently, the furnace was fast cooled to 350 °C and the crucible containing the product was taken out from the furnace. The powder thus obtained (hereafter referred to as nitrate-derived sample) was used for further characterization.

2.2. Synthesis by citrate sol–gel method

Layered $LiCo_{1/3}Mn_{1/3}Ni_{1/3}O_2$ using sol–gel method was prepared as described elsewhere [25] by taking nitrate salts of Li, Co, Ni, Mn in the molar ratio of 1.1:0.33:0.33:0.33, respectively, while using citric acid as the chelating agent. The metal to citric acid ratio for the synthesis was kept as 2:1 and the pH of the solution was raised to 10 by adding ethylene diamine. The resulting solution was heated on a hot plate at 80 °C with constant stirring to get a gel which on further heating decomposed to yield a homogeneously mixed amorphous powder containing carbon residue. The as-prepared powder was heated in a muffle furnace at 650, 800 and 1000 °C for 3 h to obtain carbon-free crystalline product.

2.3. Synthesis by combustion route

Combustion method involves exothermic redox reaction of an oxidizer (metal nitrates) and an organic fuel (oxalyl dihydrazide) to obtain the desired phase. The stoichiometry of metal nitrate to fuel was calculated assuming the complete combustion to yield metal oxide phase, and CO_2, N_2 and H_2O as by-products. The typical preparation of $LiNi_{1/3}Mn_{1/3}Co_{1/3}O_2$ by combustion synthesis was as follows. Aqueous solution of $LiNO_3$, $Co(NO_3)_2·6H_2O$, $Ni(NO_3)_2·6H_2O$ and $Mn(NO_3)_2·4H_2O$ in the molar ratio of 1.1:0.33:0.33:0.33 was mixed with stoichiometric amounts of fuel, namely oxalyl dihydrazide (ODH): nitrate in molar ratio of 1.5:1. Excess lithium was introduced to account for the lithium loss during heating. The slurry obtained was introduced to preheated furnace at 500 °C. The solution froth boils and catches fire with evolution of gases. The dark brown product thus obtained was further heated at appropriate temperatures to obtain electrochemically active phase.

X-ray diffraction patterns for the samples prepared by these three methods were recorded using X'pert PRO-PANalytical diffractometer using Cu Kα radiation. The crystal structure, lattice parameter and extent of Li/Ni cation mixing in the samples were determined by Reitveld refinement of powder X-ray diffraction data using General Structure Analysis System (GSAS) code [26]. The morphology and changes in crystallinity of the powder samples were checked with a scanning electron microscope (HITACHI Model S-3000H). Chemical analyses of the samples were carried out using PerkinElmer Atomic Absorption Spectrometer. The

positive electrode for electrochemical studies were prepared by mixing 85% active material and 15% SP carbon as conducting additive. Swagelock™ type cells were assembled and sealed in an argon-filled glove box with lithium foil as the anode and 1 M $LiPF_6$ dissolved in EC/DMC (1:1 by volume) as the electrolyte. The cells thus fabricated were cycled galvanostatically in the voltage range between 3 and 4.5 V versus lithium using VMP3Z (Biologica) multi-channel potentiostat/galvanostat.

3. Results and discussion

X-ray diffraction patterns for the $LiNi_{1/3}Mn_{1/3}Co_{1/3}O_2$ synthesized by nitrate-melt decomposition at varying temperatures, namely 750, 800, 850 and 900 °C, are shown in Fig. 1. All the patterns could be indexed on α-$NaFeO_2$ type layered structure with space group: $R\bar{3}m$. However, careful examination of the diffraction pattern for the sample heated at 750 °C (Fig. 1(d)) shows the absence of splitting (doublet) for (0 0 6)/(0 1 2) and (0 1 8)/(1 1 0) reflections indicating lack of a perfectly layered structure. All other samples obtained at temperatures >750 °C clearly exhibit splitting of these peaks in the XRD suggesting formation of the perfectly layered structure. Furthermore, the intensity ratio $I_{(0 0 3)}/I_{(1 0 4)}$ for the samples prepared at 800 °C indicates cation ordering with low degree of cation mixing [27] compared to the samples prepared at 850 and 900 °C.

As-prepared sample derived from sol–gel synthesis is amorphous with fluffy carbonaceous mass. It is further heated above 700 °C to remove the carbonaceous mass and to facilitate the formation of crystalline product. Fig. 2 shows the XRD for the sol–gel derived $LiNi_{1/3}Mn_{1/3}Co_{1/3}O_2$ samples annealed at different temperatures, namely 800 and 1000 °C. It is seen from the data that the (0 0 6)/(1 0 2) and (0 1 8)/(1 1 0) peak splitting for the sample heated at 800 °C is rather obscure suggesting that perfect α-$NaFeO_2$ structure is not obtained at 800 °C. The sol–gel sample heated at 1000 °C on the other hand showed well-defined splitting of the afore said diffraction peaks indicating the formation of the product possessing the perfectly layered structure.

X-ray diffraction patterns for the samples prepared by combustion method are shown in Fig. 3. Despite the absence of (0 0 6)/(1 0 2) and (0 1 8)/(1 1 0) peak splitting for the as-prepared sample, all the patterns could be indexed on α-$NaFeO_2$ type structure. The sample calcined at 800 °C for 2 h exhibits a single phase with a well-developed XRD pattern. But the integrated

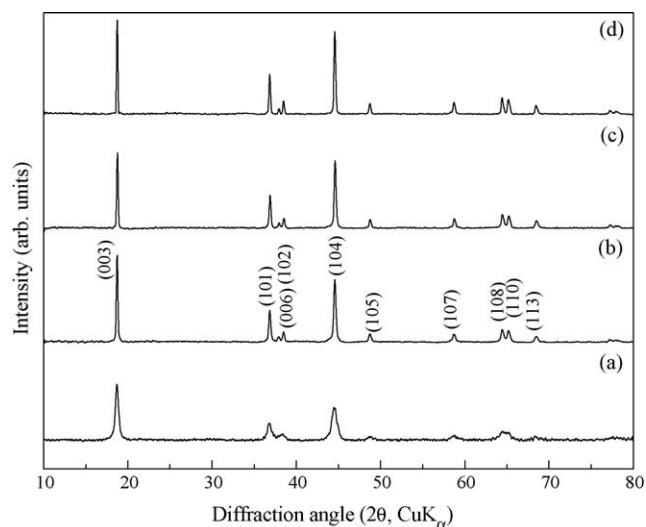**Fig. 1.** Powder X-ray diffraction patterns of $LiNi_{1/3}Mn_{1/3}Co_{1/3}O_2$ obtained by nitrates decomposition at (a) 750 °C, (b) 800 °C, (c) 850 °C and (d) 900 °C.

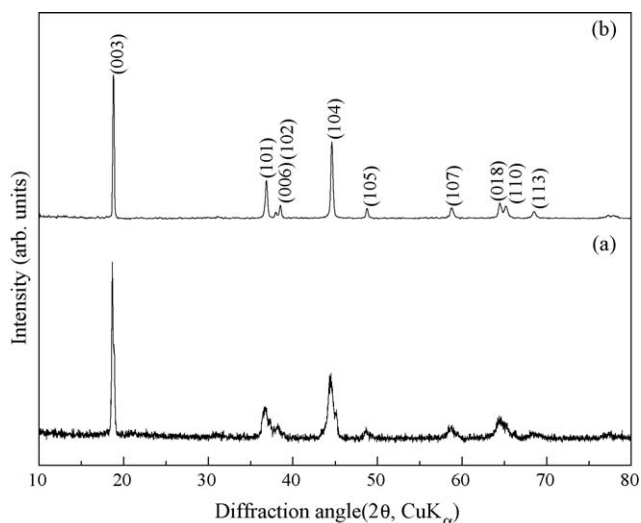**Fig. 2.** Powder X-ray diffraction patterns of $LiNi_{1/3}Mn_{1/3}Co_{1/3}O_2$ obtained by sol–gel method at (a) 800 °C and (b) 1000 °C.

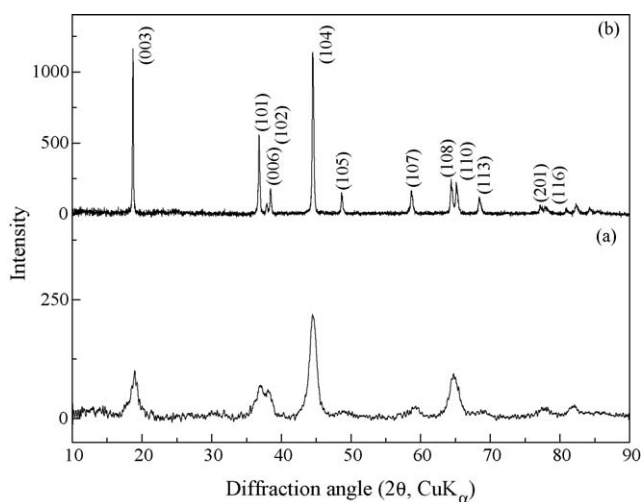**Fig. 3.** Powder X-ray diffraction patterns of $LiNi_{1/3}Mn_{1/3}Co_{1/3}O_2$ obtained by combustion method (a) as prepared (b) at 800 °C.

intensity ratio of (0 0 3) to (1 0 4) peak is 1.15, indicating undesirable cation mixing. Heating the sample above 800 °C results in decrease of (0 0 3) to (1 0 4) peaks intensity ratio to <1.1 indicating larger cation mixing at higher temperatures.

Detailed structural analyses of the diffraction patterns have been conducted to quantify the XRD data. For Reitveld analysis, we have used samples prepared at optimized conditions, namely sample synthesized by nitrate-melt decomposition at 800 °C, sol–gel synthesized sample calcined at 1000 °C and combustion-synthesized sample calcined at 800 °C. Fig. 4(a–c) presents the XRD Reitveld-fit patterns for $LiNi_{1/3}Mn_{1/3}Co_{1/3}O_2$ prepared by nitrate-melt decomposition, sol–gel and combustion method, respectively. During the refinement of the XRD data, occupancy of Co and Mn are fixed as 1/3 at 3b-sites. Initially, refinements are carried out assuming no exchange between Li and Ni cation sites, i.e. all Li atoms are kept at 3a-sites and all Ni atoms are kept at 3b-sites. The refinement converged with higher agreement factors, for example, the R_{wp} values obtained are 10.4, 9.3 and 12.5, respectively, for nitrate, sol–gel and combustion-derived samples. In the final stages of refinement, the distribution of Li- and Ni-sites between 3a-alkali metal sites and 3b-transition-metal sites is allowed to
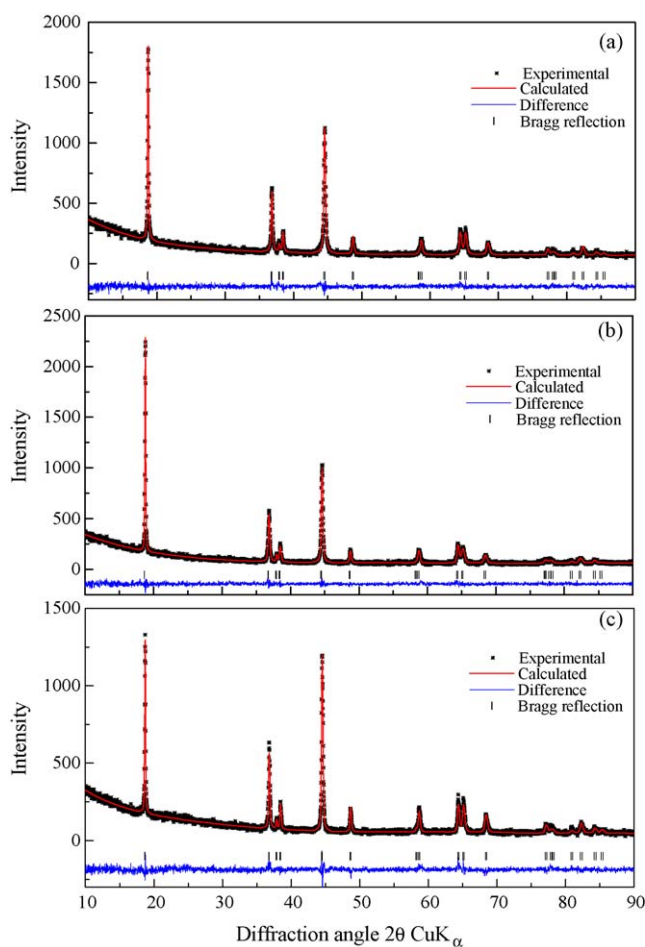

Fig. 4. XRD Reitveld fit for $LiNi_{1/3}Mn_{1/3}Co_{1/3}O_2$ derived from (a) nitrate-melt decomposition method, (b) sol–gel method and (c) combustion method.

refine keeping total (Li + Ni) content as (1 + 1/3). This improves the fit substantially and gives better agreement values. Crystallographic parameters and agreement factors (R_{wp} and χ^2) obtained by Reitveld refinement are listed in Table 1. The refinement shows that Li/Ni disorder is about 2.14, 5.39 and 9.67%, respectively, for samples derived from sol–gel, nitrate-melt decomposition and combustion methods. Furthermore, the actual concentration of metal ions in the samples are determined by atomic absorption spectroscopy and the stoichiometries thus obtained are $Li_{0.98}Ni_{0.32}Co_{0.33}Mn_{0.31}O_2$, $Li_{0.98}Ni_{0.31}Co_{0.31}Mn_{0.33}O_2$ and $Li_{0.97}Ni_{0.31}Co_{0.33}Mn_{0.32}O_2$, respectively, for as-prepared samples obtained by nitrate-melt decomposition, combustion route and sol–gel methods; these compositions are close to nominal stoichiometry.

Scanning electron microscopic studies are conducted to examine the morphology of $LiNi_{1/3}Mn_{1/3}Co_{1/3}O_2$ samples obtained

Table 1
XRD Reitveld refinement data for $LiNi_{1/3}Mn_{1/3}Co_{1/3}O_2$ prepared by various methods.

Preparation method	Nitrate-melt decomposition (800 °C)	Sol–gel (1000 °C)	Combustion (800 °C)
$a = b$	2.873 (4)	2.866 (7)	2.864 (8)
c	14.296 (19)	14.248 (3)	14.254 (4)
c/a	4.976	4.971	4.976
Li/Ni disorder	5.39 (1)	2.14 (1)	9.67 (1)
R_{wp}	8.05	8.45	9.0
χ^2	0.85	0.82	0.87

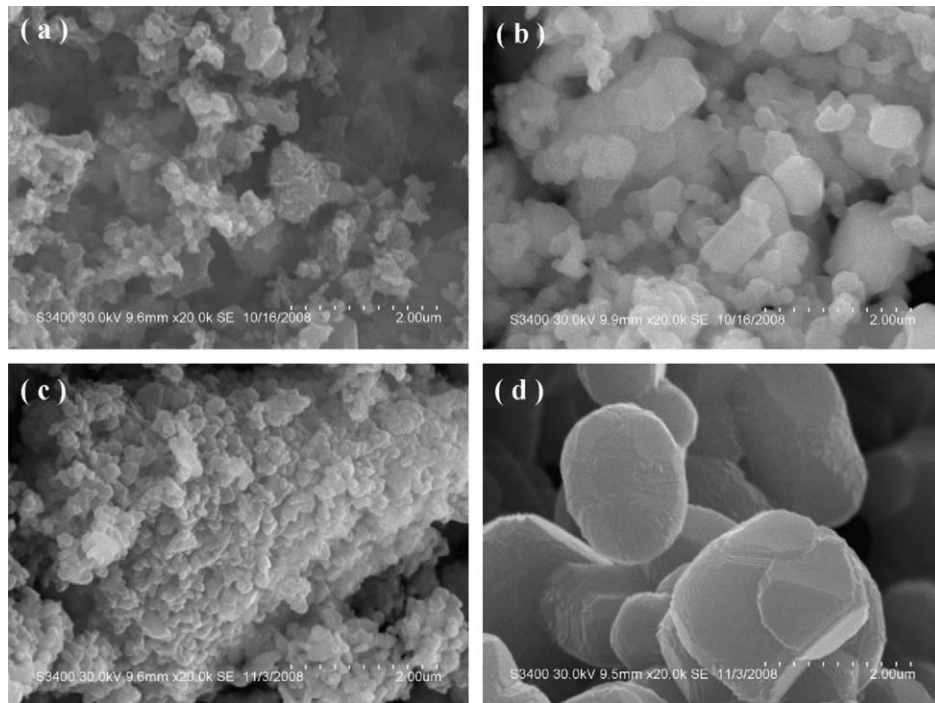**Fig. 5.** Scanning electron micrograph of $LiNi_{1/3}Mn_{1/3}Co_{1/3}O_2$ synthesized using (a) nitrate-melt decomposition method, (b) sol–gel method and (c and d) combustion method where (c) as synthesized (d) after calcination.

by three different synthetic routes, viz. nitrate-melt decomposition, sol–gel and combustion methods. SEM images of representative $LiNi_{1/3}Mn_{1/3}Co_{1/3}O_2$ samples with the same magnification are shown in Fig. 5. Nitrate-derived sample prepared at 800 °C contains agglomerates of nanometric particles of 200–300 nm. However, sol–gel derived samples prepared at 1000 °C show well-developed particles of micrometer size, typically of 0.5 μm. The as-prepared samples derived by combustion method comprise particles in the nanometric range (see Fig. 5(c)); the final product formed after heating at 800 °C has well-defined platelet like crystallites of about 1–2 μm. It is noteworthy that though 1000 °C is used for post-treatment of sol–gel derived sample, the particle sizes are still smaller than that for combustion-derived sample post-treated at 800 °C. The bigger particle size for the combustion-derived sample could be attributed to the high sinterability of the nano-particulate powders [28]. In all the three samples, distribution of Co, Ni and Mn in the individual crystallites is probed using EDAX analysis. EDAX analysis confirms that samples are homogeneous and the transition-metal cations are in the expected ratio.

From the foregoing, it is clear that $LiNi_{1/3}Mn_{1/3}Co_{1/3}O_2$ obtained by three different rapid synthetic approaches is morphologically and crystallographically different from each other. Accordingly, it is important to assess and understand their electrochemical behavior and correlate with the above observations. For this purpose, the cells with optimized samples of $LiNi_{1/3}Mn_{1/3}Co_{1/3}O_2$ are subjected to galvanostatic cycling with 1 Li in 5 h rate in the voltage range between 3 and 4.5 V. Fig. 6 shows the voltage versus composition profiles for optimized $LiNi_{1/3}Mn_{1/3}Co_{1/3}O_2$ samples prepared by nitrate-melt decomposition (800 °C), sol–gel (1000 °C) and combustion methods (800 °C). The smooth curves for charge–discharge processes for all samples show the absence of spinel-phase formation during cycling.

In the initial stages of lithium deintercalation, Ni^{2+} oxidizes to Ni^{3+} and subsequently to Ni^{4+} [29], which is equivalent to a removal of 0.66 Li (or 0.66e) corresponding to the theoretical capacity of 148 mAh/g. On further deintercalation, only a fraction

of Co^{3+} is oxidized to Co^{4+} extending the capacity value of $Li_{1-x}Ni_{1/3}Mn_{1/3}Co_{1/3}O_2$ to about 165 mAh/g. As is seen from the data in Fig. 6, the nitrate-melt-decomposed sample shows higher reversible capacity and lower polarization. A maximum of about 0.68 Li (=0.68e) can be reversibly removed for the nitrate-melt-decom-
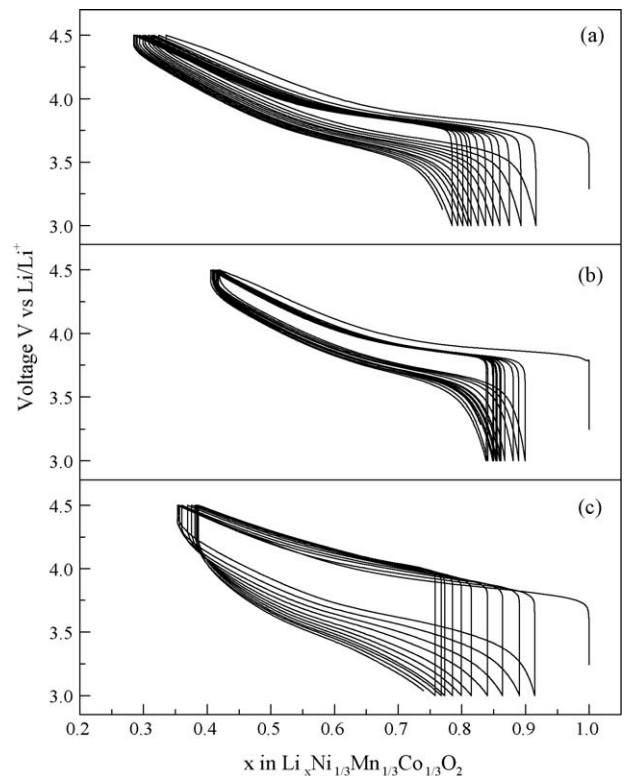

Fig. 6. Electrochemical galvanostatic cycles for $LiNi_{1/3}Mn_{1/3}Co_{1/3}O_2$ versus metallic Li at 1 Li/5 h rate prepared by (a) nitrate-melt decomposition, (b) sol–gel method and (c) combustion method.
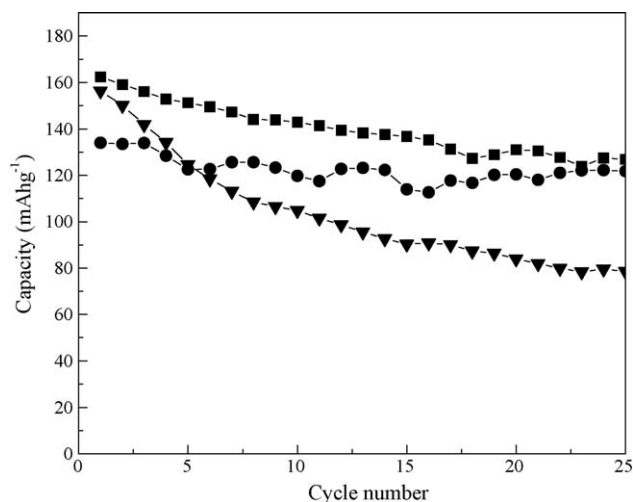
Fig. 7. Discharge capacity versus cycle number for Li/LiNi$_{1/3}$Mn$_{1/3}$Co$_{1/3}$O$_2$ cells cycled between 3 and 4.5 V at room temperature ($\sim$30 °C) with LiNi$_{1/3}$Mn$_{1/3}$Co$_{1/3}$O$_2$ prepared by (■) nitrate-melt decomposition, (●) sol–gel and (▲) combustion method.

position-derived sample during the first charge amounting to a charge capacity of 188 mAh/g. For the sol–gel derived sample, owing to the larger particle size and a larger diffusion distance for lithium ion, the charging ended prior to other two samples, reducing its initial charge/discharge capacity to 162/134 mAh/g. However, the capacity retention is better than the other samples as 91% of its capacity is retained after 25 cycles (Fig. 7). The capacity fade during cycling at higher voltages is expected due dissolution of material, phase changes, etc. The combustion-derived sample shows poor capacity retention because of the large amount of Ni^{2+}/Li$^+$ cation mixing and associated defects in the crystal structure. It loses almost 50% of its initial capacity after 25 cycles. It is therefore surmised that the nitrate-melt method not only offers the advantage of low processing temperature but also is time saving and cost effective for bulk production of oxide cathodes; it also provide cathode material with superior electrochemical performance.

4. Conclusion

Electrochemically active LiNi$_{1/3}$Mn$_{1/3}$Co$_{1/3}$O$_2$ has been prepared by three different synthetic routes namely nitrate-melt decomposition, combustion and sol–gel methods. LiNi$_{1/3}$Mn$_{1/3}$Co$_{1/3}$O$_2$ prepared by different methods has varying degrees of cation mixing, morphology, and hence exhibits significantly variant electrochemical performance. The sol–gel synthesized sample has Ni to Li exchange of only about 2% compared to 5% and 9%, respectively, for nitrate-melt decomposition and combustion-derived samples. The sol–gel synthesized sample has well-developed particles of 0.5 μm while the nitrate-derived sample contains agglomerates of nanometric particles of 200–300 nm. By contrast, the combustion-derived sample exhibits well-defined platelet-like crystallites of 1–2 μm. The resulting electrochemical behavior of LiNi$_{1/3}$Mn$_{1/3}$Co$_{1/3}$O$_2$ synthesized by three different rapid-synthesis routes is influenced by factors such as cation mixing, particle size and morphology. Overall, the nitrate-melt-decomposition-derived sample shows superior electrochemical behavior. The combustion-derived sample has maximum cation mixing among all the three methods and shows poor capacity retention.

References

[1] K. Ozawa, Solid State Ionics 69 (1994) 212.
[2] K. Mizushima, P.C. Jones, P.J. Wiseman, J.B. Goodenough, Mater. Res. Bull. 15 (1980) 783.
[3] J.M. Tarascon, M. Armand, Nature 414 (2001) 359.
[4] A. Rougier, P. Gravereau, C. Delmas, J. Electrochem. Soc. 143 (1996) 1168.
[5] A. Hirano, R. Kanno, Y. Kawamoto, Y. Takeda, K. Yamaura, M. Takano, K. Ohyama, M. Ohashi, Y. Yamaguchi, Solid State Ionics 78 (1995) 123.
[6] J.M. Tarascon, D. Guyomard, Electrochim. Acta 38 (1993) 1221.
[7] A.R. Armstrong, P.G. Bruce, Nature 381 (1996) 499.
[8] A.R. Armstrong, N. Dupre, A.J. Paterson, C.P. Grey, P.G. Bruce, Chem. Mater. 16 (2004) 3106.
[9] Y. Shao-Horn, S.A. Hackney, A.R. Armstrong, P.G. Bruce, R. Gitzendanner, C.S. Johnson, M.M. Thackeray, J. Electrochem. Soc. 146 (1999) 2404.
[10] T. Ohzuku, Y. Makimura, Chem. Lett. 30 (2001) 642.
[11] Y. Koyama, N. Yabuuchi, I. Tanaka, H. Adachi, T. Ohzuku, J. Electrochem. Soc. 151 (2004) A1545.
[12] L. Sebastian, J. Gopalakrishnan, J. Mater. Chem. 13 (2003) 433.
[13] J.-M. Kim, H.-T. Chung, Electrochim. Acta 49 (2004) 937.
[14] D.-C. Li, T. Muta, L.-Q. Zhang, M. Yoshio, H. Noguchi, J. Power Sources 132 (2004) 150.
[15] P. He, H. Wang, L. Qi, T. Osaka, J. Power Sources 160 (2006) 627.
[16] X. Li, Y.J. Wei, H. Ehrenberg, F. Du, C.Z. Wang, G. Chen, Solid State Ionics 178 (2008) 1969.
[17] Y.-S. He, Z.-F. Ma, X.-Z. Liao, Y. Jiang, J. Power Sources 163 (2007) 1053.
[18] Y. Fujii, H. Miura, N. Suzuki, T. Shoji, N. Nakayama, J. Power Sources 171 (2007) 894.
[19] N. Yabuuchi, T. Ohzuku, J. Power Sources 119–121 (2003) 171.
[20] J. Guo, L.F. Jiao, H.T. Yuan, H.X. Li, M. Zhang, Y.M. Wang, Electrochim. Acta 51 (2006) 3731.
[21] K.M. Shaju, G.V. Subba Rao, B.V.R. Chowdari, Electrochim. Acta 48 (2002) 145.
[22] T.H. Cho, S.M. Park, M. Yoshia, T. Hirai, Y. Hideshima, J. Power Sources 142 (2005) 306.
[23] M. Sathiya, A.S. Prakash, K. Ramesha, A.K. Shukla, *Materials* (2009), (In print).
[24] G.A. Nazri, G.C. Garabedian, United States Patent US 7,018,607 B2.
[25] P. Samarasingha, D.-H. Tran-Nguyen, M. Behm, A. Wijayasinghe, Electrochim. Acta 53 (2008) 7995.
[26] A.C. Larson, R.B. Van Dreele, Los Alamos National Laboratory Report No. LAUR 86-748 (2000); B.H. Toby, J. Appl. Crystallogr. 34 (2001) 210.
[27] P. Reale, D. Privitera, S. Panero, B. Scrosati, Solid State Ionics 178 (2007) 1390.
[28] R.D. Purohit, S. Saha, A.K. Tyagi, Ceram. Int. 32 (2006) 143.
[29] Y. Koyama, I. Tanaka, H. Adachi, Y. Makimura, T. Ohzuku, J. Power Sources 119–121 (2003) 644.